Stochastic Environmental Research and Risk Assessment (2025) 39:1345–1358
https://doi.org/10.1007/s00477-025-02916-2

ORIGINAL PAPER

Covariance models through difference between Matérn families

D. Posa[1]

Accepted: 15 January 2025 / Published online: 26 February 2025

Abstract
It is well known that Whittle–Matérn family represents one of the most utilized class of covariance functions because of some special features which are capable to describe several correlation structures. However, one of the main drawbacks of this last family concerns its failure to model negative correlation structures. In this paper, utilizing the Whittle–Matérn family, new classes of covariance models, suitable to model negative correlations, have been presented and their properties have been analyzed. The new families are flexible enough because they allow to choose covariance models which always present positive values in their domain, as well as covariance models which are negative in a subset of their domain. On the other hand, all the traditional hole effect models, proposed in the literature, essentially stem from the Bessel family and they are characterized by the same features, i.e., they present a countable infinity of zeros and a parabolic behaviour near the origin. Conversely, the models proposed in this paper are characterized by a complementary behaviour, which cannot be detailed by all the classical hole effect correlation models: they are essentially characterized by just one zero, moreover they are able to describe various behaviours near the origin (linear and parabolic), as well as different behaviours concerning the concavity in proximity of the origin (upwards and downwards). In summary, they can describe correlation structures which cannot be detailed by the Whittle–Matérn family.

Keywords Covariance functions · Spectral density function · Negative correlation

1 Introduction

Whittle–Matérn class (Matérn 1980) is a flexible parametric family capable to describe several spatial correlation structures: indeed, this class of covariance models is appropriate to analyze a large set of behaviors thanks to the parameters, which control the range of correlation as well as the smoothness of the random function. The exponential model and the model introduced by Whittle (1954), commonly used in hydrology (Meija and Rodriguez-Iturbe 1974; Jones 1989; Creutin and Obled 1982) for two-dimensional random fields, represent some special cases. On the other hand, it is well known (Handcock and Stein 1993) that the Gaussian covariance function (c.f.) represents a special case of this class, when the smoothness parameter goes to infinity.

Guttorp and Gneiting (2006) gave a summary of the important properties of the Whittle–Matérn family and a detailed discussion of its history. Several contributions on this last class of models can be found in Apanasovich and Genton (2010), Apanasovich et al. (2012), Guinness (2022); in particular, Lindgren et al. (2011) detailed the connections between stochastic partial differential equations and Matérn family.

Although the Whittle–Matérn family of c.f.s is admissible in any dimensional space, however the same class presents some severe drawbacks: indeed, it is strictly decreasing and it is always positive (Stein 1999), for these reasons it forecloses the possibility to model negative correlation structures.

In most of the applications negative correlation is often described through hole effect models or damped oscillation models, as detailed by various authors (Ma and Jones 2001; Journel and Froidevaux 1982; Asghari 2015). Apart from the just mentioned geological and mining applications, in the last years hole effect models have been employed to describe the fluctuating spatial structure of functional magnetic resonance imaging data to enhance the detection of

✉ D. Posa
donato.posa@unisalento.it

[1] Dipartimento di Scienze Economiche e Matematico-Statistiche, University of Salento, Complesso Ecotekne, Via per Monteroni, Lecce, Italy

activated brain regions, considering both the nonlinear physical relationship between the proximate voxels and the functional relationship between distant voxels (Ye et al. 2015). However, it is suitably to underline that all the traditional hole effect models essentially stem from the Bessel family and they are characterized by the same features, i.e., they present a countable infinity of zeros and a parabolic behaviour near the origin. As a consequence, c.f.s characterized by just one zero and a linear behaviour near the origin cannot be described by the family of the hole effect models.

C.f.s with negative values can be encountered in various applications, as underlined by various authors (Pomeroy et al. 2003; Xu et al. 2003b; Levinson et al. 1984; Yakhot et al. 1989; Shkarofsky 1968; Xu et al. 2003a). One particular example characterized by negative correlation, involving the Gaussian and Matérn family, has been given in Gregori et al. (2008). A special family of infinitely differentiable Bessel-Lommel c.f.s that always exhibit an hole effect and are valid in $\mathbb{R}^m$, where $m > 2$, was derived by Hristopulos (2015), although the exact functional form of these c.f.s is not exactly the same for different dimensions. The permissibility for the linear combinations of two real spatial or spatio-temporal c.f.s (or variograms) isotropic in space, in all dimensions, has been investigated by Ma (2005): it was found out that the resultant covariance may be just available in certain finite dimensions if one of the coefficients of the linear combinations is negative. Recently a hybrid spectral approach for generating covariance kernels which is based on physical arguments has been presented in Hristopulos (2024); in particular, some covariance models characterized by negative values have been provided. Moreover, in Hristopulos (2024) it has been proved that a scale-dependent family of c.f.s, obtained as a reparameterization of the Generalized Cauchy family, converges to a particular case of the Matérn family. Further up to date contributions and development concerning Whittle–Matérn family can be found in Faouzi et al. (2022), Porcu et al. (2024), Wang et al. (2023). On the other hand, Alegria et al. (2024) recently have derived a hybrid Cauchy-Matérn model, which allows to index both long memory and mean square differentiability of the random field, and a hybrid hole effect Matérn model which is capable of attaining negative values (hole effect) while preserving the local attributes of the traditional Matérn model.

A negative correlation in time series analysis can be found in the field of agriculture and in financial data, characterized by high frequency, whereas in spatial data analysis negative correlation can be found in medical, biological and physical problems (Griffith 2019; Hu et al. 2018).

The main aim of this paper is to provide a further development and generalization, valid for any dimension *m* of the Euclidean space $\mathbb{R}^m$, of the results given in Posa (2023), in order to utilize the Whittle–Matérn class with the purpose to get c.f.s able to describe negative correlation models. As already underlined, most of the classical hole effects covariance families present several limitations for modelling negative correlations structures. Utilizing a general recent result (Posa 2021), conditions under which the difference between two c.f.s belonging to the Whittle–Matérn family is still a c.f., have been explored, together with their flexible and broad range properties: indeed, the models proposed in this paper are characterized by a complementary behaviour, which cannot be detailed by all the classical hole effect correlation models. In particular, they can assume negative and/or positive values by appropriately adapting the values of the parameters and they are characterized by just one zero. Moreover, this new family of c.f.s is able to describe various behaviours in a neighborhood of the origin; at this purpose, some c.f.s can present a linear behaviour with downwards concavity, which cannot be described by the Whittle–Matérn class of models: for example, the exponential model, which belongs to the Whittle–Matérn class, is characterized by a linear behaviour and upwards concavity near the origin, whereas the Gaussian model, which also belongs to the same class, presents a parabolic behaviour and downwards concavity in a neighborhood of the origin.

In order to underline that the admissibility of a c.f. strongly depends on the dimension *m* of the Euclidean space $\mathbb{R}^m$ in which the same c.f. is defined, it will be detailed that, most of the times, this relevant aspect is forgotten; at this purpose, the various examples described in Ma and Jones (2001) are not valid in $\mathbb{R}^2$ or $\mathbb{R}^3$.

The results of this paper are essentially devoted to isotropic c.f.s: please note that these particular families are the basis to construct anisotropic c.f.s; moreover, isotropic c.f.s cover a significant role in the theory of turbolence (Batchelor 1982), on the behaviour of ocean waves (Longuet-Higgins 1957) and road roughness modelling (Kamash and Robson 1978).

This paper is divided in the following parts: in Sect. 2, some peculiarities of isotropic c.f.s are described, in particular the Whittle–Matérn class of c.f.s has been briefly treated, together with some results on this class of models. In Sect. 3 the new families of c.f.s have been introduced, whereas in Sect. 4 a parametric analysis on these new classes and some relevant results have been given and properly represented. The outputs of this kind of analysis are particularly flexible and useful for many practitioners.

2 A brief overview on isotropic covariance functions and Whittle–Matérn family

In the present section a brief outline on isotropic c.f.s and on Whittle–Matérn family has been provided. In the literature, the standard results on isotropic c.f.s and on Whittle–Matérn family, given herafter, can be found in various textbooks and papers (Handcock and Stein 1993; Hristopulos 2020; Schoenberg 1938; Yaglom 1987).

2.1 Isotropic covariance functions

Bochner's theorem (Bochner 1959) completely characterizes any continuous c.f.; indeed

$$C : \mathbb{R}^m \to \mathbb{C},$$

where $\mathbb{R}^m$ is the m-dimensional Euclidean space and $\mathbb{C}$ is the set of the complex numbers, is a c.f. if and only if it can be expressed as follows:

$$C(\mathrm{s}) = \int_{\mathbb{R}^m} \exp(i\boldsymbol{\omega}^T \mathrm{s}) dF(\boldsymbol{\omega}), \tag{1}$$

where i is the imaginary unit and F is a finite and non decreasing measure.
If the measure F is absolutely continuous, then:

$$C(\mathrm{s}) = \int_{\mathbb{R}^m} \exp(i\boldsymbol{\omega}^T \mathrm{s}) f(\boldsymbol{\omega}) d\boldsymbol{\omega}, \tag{2}$$

where the function f, usually called spectral density (s.d.), is non negative and $f \in L^1(\mathbb{R}^m)$.
If $C \in L^1(\mathbb{R}^m)$, then:

$$f(\boldsymbol{\omega}) = \frac{1}{(2\pi)^m} \int_{\mathbb{R}^m} \exp(-i\boldsymbol{\omega}^T \mathrm{s}) C(\mathrm{s}) d\mathrm{s}, \tag{3}$$

and f is continuous.
If C is isotropic, i.e., $C(\mathrm{s}) = C(s)$, where $s = ||\mathrm{s}|| = \sqrt{\sum_{i=1}^m s_i^2}$, hence a real function, and

$$\int_0^\infty s^{m-1} |C(s)| ds < \infty, \quad m \in \mathbb{N}, \quad m \geq 2,$$

then:

$$C(s) = (2\pi)^{m/2} \int_0^\infty \frac{J_{(m/2-1)}(ws)}{s^{(m/2-1)}} w^{m/2} f(w) dw, \quad s > 0, \tag{4}$$

where J is a Bessel function of order $(m/2-1)$. In this case, the expression of the s.d. function is given hereafter:

$$f(w) = \frac{1}{(2\pi)^{m/2}} \int_0^\infty \frac{J_{(m/2-1)}(ws)}{w^{(m/2-1)}} s^{m/2} C(s) ds. \tag{5}$$

In the literature there exist relevant results for isotropic c.f.s which rely on completely monotone and Bessel functions (Schoenberg 1938; Polya 1949; Yaglom 1987).

2.2 The Whittle–Matérn family

In this section a brief overview on the Whittle–Matérn family, well known in the literature (Handcock and Stein 1993; Matérn 1980), has been given. In particular, the class of Whittle–Matérn c.f.s is given hereafter:

$$C(s; \lambda, \nu) = AD(\lambda s, \nu), \quad A > 0, \nu > 0, \lambda > 0, \tag{6}$$

where $D(L, \nu) = L^\nu K_\nu(L)$, K_ν is the modified Bessel function of second kind, λ and ν are, respectively, a scale parameter and a smoothness parameter and $L = \lambda s$. The above class of c.f.s is admissible in any dimensional space. One of the general expression of the function K_ν in (6) is given hereafter:

$$K_\nu(s; \lambda) = \frac{\Gamma(\nu + 1/2)(2s)^\nu}{\sqrt{\pi}\lambda^\nu} \int_0^\infty \frac{cos(t\lambda)}{(t^2 + s^2)^{\nu+1/2}} dt, \tag{7}$$

and the s.d. f of the Whittle–Matérn class is also provided:

$$f(w; \lambda, \nu) = \chi \frac{2^{(\nu-1)}}{(\pi)^{m/2}} \frac{\Gamma(\nu + m/2)\lambda^{2\nu}}{(w^2 + \lambda^2)^{\nu+m/2}}, \qquad \chi > 0. \tag{8}$$

If $\nu = n + 1/2, n \in \mathbb{N}$, then the Whittle–Matérn family is simply the product of a polynomial of order n with an exponential, as specified hereafter:

$$C(s; n + 1/2) = \\ = \exp\left(\frac{-\sqrt{2n+1} \cdot s}{\rho}\right) \frac{n!}{(2n)!} \sum_{i=0}^{n} \frac{(n+i)!}{i!(n-i)!} \left(\frac{2\sqrt{2n+1} \cdot s}{\rho}\right)^{n-i}, \tag{9}$$

where $\lambda = \frac{\sqrt{2n+1}}{\rho}$. Some simple expressions, for some values of the integer n, are given below (Hristopulos 2020):

- $\nu = 1/2, \quad n = 0,$

$$K_{1/2}(L) = \frac{\sqrt{2\pi} e^{-L}}{2\sqrt{L}}, \qquad C(L; 1/2) = L^{1/2} K_{1/2}(L);$$

- $\nu = 3/2, \quad n = 1,$

$$K_{3/2}(L) = \frac{\sqrt{2\pi}}{2}(L+1)\frac{e^{-L}}{L^{3/2}}, \qquad C(L; 3/2) = L^{3/2} K_{3/2}(L);$$

- $\nu = 5/2, \quad n = 2,$

$$K_{5/2}(L) = \frac{\sqrt{2\pi}}{2}(L^2 + 3L + 3)\frac{e^{-L}}{L^{5/2}},$$
$$C(L; 5/2) = L^{5/2}K_{5/2}(L).$$

Lemma 1 Let $f(s) = P_n(s) \cdot \exp(-as), a > 0, s \geq 0$, where

$$P_n(s) = \sum_{i=0}^{n} a_i s^i, \qquad n \geq 1,$$

then the function f shows a behaviour which is parabolic in proximity of the origin if:

$$a_1 = a \cdot a_0.$$

Proof Note that $f'(s) = \exp(-as) \cdot [P_n'(s) - aP_n(s)]$, hence $f'(0) = 0 \Longleftrightarrow a_1 = a \cdot a_0$.
□

Corollary 1 The subset of the Whittle–Matérn family given in (9) displays a behaviour which is parabolic in a neighborhood of the origin if $n \geq 1$.

Proof Note that in (9) $a = \frac{\sqrt{2n+1}}{\rho}, \quad a_0 = 1 \quad a_1 = \frac{\sqrt{2n+1}}{\rho}$; hence, according to Lemma 1, it is straightforward to show that $a_1 = a \cdot a_0$.
□

As already underlined in the Introduction, the Whittle–Matérn family converges to the Gaussian c.f. as $\nu \to \infty$ in (6).

Different applications concerning field temperature, wind field, soil and sea beam data utilize the Whittle–Matérn family because of its flexibility for modelling various correlation structures. However, as specified before, a significant restriction of Whittle–Matérn c.f.s concerns their failure to model negative correlations, because the same family is always positive in any dimensional space.

3 Covariance models through differences between Matérn families

The overall question which involves the difference between complex c.f.s has been discussed in Posa (2021).

In this section, taking into account these last results, some relevant and useful outcomes concerning the difference of Matérn c.f.s will be provided. The resulting families of c.f.s, achieved through the above difference, are characterized by various behaviours in proximity of the origin, in addition to the fact that can present negative and/or positive values accordingly to the parameters which characterize the same class. In particular, these results can be considered a further development and a generalization of the ones obtained in Posa (2023).

Theorem 1 Let $C_k, k = 1, 2$ be Whittle–Matérn c.f.s as in (6) and consider

$$C(s; \boldsymbol{\Theta}) = AD_1(L_1, \nu_1) - BD_2(L_2, \nu_2), \quad A > 0, B > 0, \quad \boldsymbol{\Theta} = (A, B, \lambda_1, \lambda_2, \nu_1, \nu_2), \tag{10}$$

where:

$$D_i(L_i, \nu_i) = \\ = (2\pi)^{m/2} \int_0^\infty \frac{J_{(m/2-1)}(ws)}{s^{(m/2-1)}} w^{m/2} f_i(w; \lambda_i, \nu_i) dw, \quad i = 1, 2,$$

with

$$f_i(w; \lambda_i, \nu_i) = \frac{f(w; \lambda_i, \nu_i)}{\chi}, \quad i = 1, 2,$$

and the s.d. f already defined in (8).
Then C defined as in (10) is a c.f. if and only if:

$$G(w; \boldsymbol{\Theta}) = \\ = \frac{A}{B} \frac{2^{(\nu_1 - 1)}}{2^{(\nu_2 - 1)}} \frac{\Gamma(\nu_1 + m/2)}{\Gamma(\nu_2 + m/2)} \frac{\lambda_1^{2\nu_1}}{\lambda_2^{2\nu_2}} \frac{(w^2 + \lambda_2^2)^{\nu_2 + m/2}}{(w^2 + \lambda_1^2)^{\nu_1 + m/2}} > 1, \quad \forall w \in \mathbb{R}_+. \tag{11}$$

Proof Note that

$$C(s; \boldsymbol{\Theta}) = \\ = (2\pi)^{m/2} \int_0^\infty \frac{J_{(m/2-1)}(ws)}{s^{(m/2-1)}} w^{m/2} [Af_1(w; \lambda_1, \nu_1) - Bf_2(w; \lambda_2, \nu_2)] dw,$$

where $(Af_1 - Bf_2)$ is integrable, since f_1 and f_2 are integrable, hence C is a c.f. if and only if $(Af_1 - Bf_2)$ is a s.d. function, i.e.,

$$(Af_1 - Bf_2) > 0 \quad \Longleftrightarrow \quad G(w; \boldsymbol{\Theta}) > 1.$$

□

Remark. A necessary condition in order to verify this last inequality is that: $\nu_2 \geq \nu_1$, otherwise if $\nu_2 < \nu_1$ then:

$$\lim_{w \to \infty} G(w; \boldsymbol{\Theta}) = 0.$$

Some special cases of the previous Theorem are given hereafter. At this purpose, in order to lighten the mathematical formalism concerning the next results, let's define:

$$R = A/B, \quad l_1 = \lambda_1/\lambda_2, \quad l_2 = \lambda_2/\lambda_1,$$
$$d_1 = \lambda_1 - \lambda_2, \quad d_2 = \lambda_2 - \lambda_1.$$

Corollary 2 From Theorem 1, if $\nu_1 = \nu_2 = \nu$, then (10) is a c.f. if and only if:

$$R > {l_2}^{2\nu}\left(\frac{w^2+\lambda_1^2}{w^2+\lambda_2^2}\right)^{\nu+m/2} \quad \forall w \in \mathbb{R}_+; \tag{12}$$

in particular, if:

$$l_2 > 1 \quad \Rightarrow \quad 1 < {l_2}^{2\nu} < R, \tag{13}$$

if:

$$l_1 > 1 \quad \Rightarrow \quad 1 < {l_1}^{m} < R. \tag{14}$$

Corollary 3 From Theorem 1, if $l_1 = l_2 = 1$, then (10) is a c.f. if and only if:

$$R > \frac{\Gamma(\nu_2+m/2)}{\Gamma(\nu_1+m/2)} 2^{\nu_2-\nu_1} \iff$$
$$\iff R > (m+2n_2-1)(m+2n_2-3)\cdots(m+2n_1+1), \tag{15}$$

taking into account the properties of Γ function, with $\nu_2 = n_2 + 1/2$, $\nu_1 = n_1 + 1/2$ and $n_2 > n_1$.
Note that inequality (13) is independent from the dimension m of the Euclidean space $\mathbb{R}^m$, unlike inequalities (14) and (15).

Remark. Of course, if $B = 0$ or if $l_1 = l_2 = 1, \nu_1 = \nu_2$ and $R > 1$ in (10), then the standard Whittle–Matérn class is obtained.

3.1 Some families of isotropic covariance functions with $\nu_1 = \nu_2$

In this section, some special cases of Corollary 2 have been considered, in particular, some special classes of c.f.s have been selected, i.e, c.f.s as in (9), obtained as the product of a polynomial with an exponential, as well as the Gaussian c.f. which is a particular element of the Matérn family, as already underlined; specifically, some models with the same parameter ν have been chosen.

Corollary 4 Assigned the isotropic exponential c.f.s in $\mathbb{R}^m$:

$$C_1(L_1) = \exp(-L_1), \quad C_2(L_2) = \exp(-L_2),$$
$$\lambda_i > 0, \; L_i = \lambda_i s, \qquad i = 1, 2,$$

corresponding to $n = 0$ in Eq. (9), then the function defined hereafter

$$C(L_1, L_2; A, B) = A\exp(-L_1) - B\exp(-L_2), \quad A > 0, B > 0, \tag{16}$$

is an isotropic c.f. in any dimensional space $\mathbb{R}^m$ if and only if:

$$1 < l_2 \le R \quad or \quad 1 < l_1 < R^{1/m}. \tag{17}$$

Proof As previously specified, note that the exponential c.f. is a particular case of the Whittle–Matérn class ($\nu = 1/2$), hence in accordance with Corollary 2, (16) is a c.f. if and only if

$$1 < l_2 \le R \quad or \quad 1 < l_1 < R^{1/m}.$$

□

Corollary 5 Assigned the following isotropic c.f.s in $\mathbb{R}^m$:

$$C_1(L_1) = (L_1+1)\exp(-L_1), \quad C_2(L_2) = (L_2+1)\exp(-L_2),$$
$$\lambda_1 > 0, \lambda_2 > 0,$$

corresponding to $n = 1$ in Eq. (9), then the function defined hereafter

$$C(L_1, L_2; A, B) = A(L_1+1)\exp(-L_1) - B(L_2+1)\exp(-L_2), \quad A > 0, B > 0, \tag{18}$$

is an isotropic c.f. in any dimensional space $\mathbb{R}^m$ if and only if:

$$1 < {l_2}^3 \le R \quad or \quad 1 < l_1 < R^{1/m}. \tag{19}$$

Proof As previously specified, both the c.f.s C_1 and C_2 are special cases of the Whittle–Matérn family ($\nu = 3/2$), hence in accordance with Corollary 2, (18) is a c.f. if and only if

$$1 < {l_2}^3 \le R \quad or \quad 1 < l_1 < R^{1/m}.$$

□

Taking into account that for $\nu \to \infty$ the difference between elements of the Matérn family corresponds to the difference between two Gaussian c.f.s as a function of the argument (λs) as detailed in (6), the following result can be provided.

Corollary 6 Assigned the isotropic Gaussian c.f.s:

$$C_1(L_1) = \exp(-L_1^2), \quad C_2(L_2) = \exp(-L_2^2), \quad \lambda_1 > 0, \lambda_2 > 0,$$

corresponding to $\nu \to \infty$ in Eq. (9), then the function defined hereafter

$$C(L_1, L_2; A, B) = A\exp\left(-L_1^2\right) - B\exp\left(-L_2^2\right), \quad A > 0, B > 0, \tag{20}$$

is a c.f. if and only if:

$$1 < l_1 < R^{1/m}. \tag{21}$$

Proof According to Corollary (2), the family (20) is a valid class of c.f.s if and only if:

$$R\left[{l_1}^2\left(\frac{w^2+\lambda_2^2}{w^2+\lambda_1^2}\right)\right]^{\nu}\left(\frac{w^2+\lambda_2^2}{w^2+\lambda_1^2}\right)^{m/2} > 1, \quad \forall w \in \mathbb{R}_+. \tag{22}$$

Since $\nu \to \infty$, then the previous inequality can be satisfied if $l_1 > 1$; as a consequence, according to Corollary (2), $1 < l_1 < R^{1/m}$.
□

All the results of this section, which can be very useful for practitioners for selecting appropriate correlation models, are summarized in Table 1.

3.2 Some classes of isotropic covariance functions with $\lambda_1 = \lambda_2$

In this section, some special cases of Corollary 3 have been considered, in particular, some classes of c.f.s have been selected, i.e, c.f.s as in (9), obtained as the product of a polynomial with an exponential, specially, some models with the same parameter λ.

Corollary 7 Assigned the following isotropic c.f.s in $\mathbb{R}^m$:

$$C_1(L) = \exp\left(-L\right), \quad C_2(L) = (L+1)\exp\left(-L\right), \quad L = \lambda s, \quad \lambda > 0,$$

corresponding to $n = 0$ and $n = 1$, respectively in Eq. (9), then the function defined hereafter

$$C(L; A, B) = A\exp\left(-L\right) - B(L+1)\exp\left(-L\right), \quad A > 0, B > 0, \tag{23}$$

is an isotropic c.f. in any dimensional space $\mathbb{R}^m$ if and only if:

$$R > m + 1. \tag{24}$$

Proof The c.f.s C_1 and C_2 previously defined, are particular cases of the Whittle–Matérn class with $\nu = 1/2$ and $\nu = 3/2$, respectively; hence in accordance with Corollary 3, (23) is a c.f. if and only if:

$$R > 2 \cdot \frac{\Gamma(3/2 + m/2)}{\Gamma(1/2 + m/2)} \iff R > m + 1;$$

in particular, if $m = 1$ then $R > 2$, if $m = 2$ then $R > 3$, if $m = 3$ then $R > 4$.
□

Corollary 8 Assigned the following isotropic c.f.s in $\mathbb{R}^m$:

$$C_1(L) = \exp\left(-L\right), \quad C_2(L) = (L^2+3L+3)\exp\left(-L\right), \quad L = \lambda s, \quad \lambda > 0,$$

corresponding to $n = 0$ and $n = 2$, respectively in Eq. (9), then the function defined hereafter

$$C(L; A, B) = A\exp\left(-L\right) - B(L^2+3L+3)\exp\left(-L\right), \quad A > 0, B > 0, \tag{25}$$

is an isotropic c.f. in any dimensional space $\mathbb{R}^m$ if and only if:

$$R > (m+1)(m+3). \tag{26}$$

Proof The c.f.s C_1 and C_2 previously defined, are particular cases of the Whittle–Matérn class with $\nu = 1/2$ and $\nu = 5/2$, respectively, hence in accordance with Corollary 3, (24) is a c.f. if and only if:

$$R > 4 \cdot \frac{\Gamma(5/2 + m/2)}{\Gamma(1/2 + m/2)} \iff R > (m+1)(m+3);$$

Table 1 Summary of the results in Sect. 3.1, with the same ν, where $\boldsymbol{\Phi} = (A, B)$

$C(L_1, L_2; \boldsymbol{\Phi})$	$Ae^{-L_1} - Be^{-L_2}$	$Ae^{-L_1^2} - Be^{-L_2^2}$	$A(L_1+1)e^{-L_1} - B(L_2+1)e^{-L_2}$
C is a c.f	$1 < l_2 \le R$, or $1 < l_1 < R^{1/m}$	$1 < l_1 < R^{1/m}$	${l_2}^3 \le R$, or $1 < l_1 < R^{1/m}$
L. B	$1 < l_2 < R$, or $1 < l_1 < R^{1/m}$		
P.B	$1 < l_2 = R$,	$1 < l_1 < R^{1/m}$	${l_2}^3 \le R$, or $1 < l_1 < R^{1/m}$
$C(L_1, L_2; \boldsymbol{\Phi}) > 0$	$1 < l_2 \le R$		${l_2}^3 \le R$
$C(L_1, L_2; \boldsymbol{\Phi}) < 0$	$1 < l_1 < R^{1/m}$	$1 < l_1 < R^{1/m}$	$1 < l_1 < R^{1/m}$

L. B. Linear Behaviour, *P.B.* Parabolic Behaviour

in particular, if $m = 1$ then $R > 8$, if $m = 2$ then $R > 15$, if $m = 3$ then $R > 24$.
□

Corollary 9 Given the following isotropic c.f.s in $\mathbb{R}^m$:

$$C_1(L) = (1+L)\cdot\exp(-L), \quad C_2(L) = (L^2+3L+3)\exp(-L), \quad L = \lambda s, \quad \lambda > 0,$$

corresponding to $n = 1$ and $n = 2$, respectively in Eq. (9), then the following function

$$C(L; A, B) = A(1+L)\cdot\exp(-L) - B(L^2+3L+3)\exp(-L), \quad A > 0, B > 0, \tag{27}$$

is an isotropic c.f. in any dimensional space $\mathbb{R}^m$ if and only if:

$$R > m + 3. \tag{28}$$

Proof The c.f.s C_1 and C_2 previously defined, are particular cases of the Whittle–Matérn class with $\nu = 3/2$ and $\nu = 5/2$, respectively, hence in accordance with Corollary 3, (27) is a c.f. if and only if:

$$R > 2\cdot\frac{\Gamma(5/2+m/2)}{\Gamma(3/2+m/2)} \quad \Longleftrightarrow \quad R > m+3;$$

in particular, if $m = 1$ then $R > 4$, if $m = 2$ then $R > 5$, if $m = 3$ then $R > 6$.
□
All the results of this section, which can be very useful for practitioners for selecting appropriate correlation models, are summarized in Table 2.

4 Main results and their representation

By considering the differences between two c.f.s, each of them given by the product of a polynomial with an exponential, different situations have been analyzed, according to the particular cases with the same values of the parameters ν and λ, respectively, as shown in the Corollaries 2 and 3 proved in the previous section.

One of the main significant aspects stemming from the results involving the difference between two Whittle–Matérn c.f.s, involves the hugely set of situations which these families are able to portray. These specific issues have been suitably analyzed, such as the behaviour near the origin, which is strongly related to the regularity of the variable under study (Chilès and Delfiner 1999; Stein 1999) as well as the flexibility of a c.f. to be able to model positive or negative correlation structures.

- Considering the class of c.f. defined in (16), if $1 < l_2 < R$ the same family displays a behaviour which is linear in a neighborhood of the origin because:

$$\lim_{s\to 0^+} C'(s) = -\lambda_1 A + \lambda_2 B < 0.$$

Moreover, if $1 < l_2 \le R$, then

$$C''(s) = \lambda_1^2 A\exp(-\lambda_1 s) - \lambda_2^2 B\exp(-\lambda_2 s),$$

hence there exists the following point of inflection

$$s_F = \frac{1}{d_2}\ln\left(\frac{l_2^2}{R}\right), \qquad if \quad \frac{l_2^2}{R} > 1;$$

from the computation of the second derivative, if $1 < \sqrt{R} < l_2 < R$ there exists downwards concavity for $0 < s < s_F$, otherwise if $1 < l_2 < \sqrt{R}$ the same family always shows upwards concavity, hence there isn't any inflection point. Furthermore, if $1 < l_2 = R$, the c.f. shows a behaviour which is parabolic in a neighborhood of the origin because: $\lim_{s\to 0^+} C'(s) = 0$.

The c.f. (16) displays negative values if: $d_2|s| < \ln\left(\frac{1}{R}\right)$; however, if $l_1 < 1$ then $1 < l_2 < R$, as a consequence the c.f. (16) always displays positive values. If $l_1 > 1$, then: $1 < l_1 < R^{1/m}$. In the present case, it is straightforward to prove that the c.f. (16) assumes negative values for all $s \in \mathbb{R}$ such that $d_1|s| > \ln R$; then, the c.f. vanishes in s_0, where:

Table 2 Summary of the results in Sect. 3.2, with the same λ, where $\mathbf{\Phi} = (A, B)$

$C(L;\mathbf{\Phi})$	$Ae^{-L} - B(L+1)e^{-L}$	$Ae^{-L} - B(L^2+3L+3)e^{-L}$	$A(L+1)e^{-L} - B(L^2+3L+3)e^{-L}$
C is a c.f	$R > m+1$	$R > (m+1)(m+3)$	$R > m+3$
L. B	$R > m+1$	$R > (m+1)(m+3)$	
P.B			$R > m+3$
$C(L;\mathbf{\Phi}) > 0$			
$C(L;\mathbf{\Phi}) < 0$	$R > m+1$	$R > (m+1)(m+3)$	$R > m+3$

L. B. Linear Behaviour, *P.B.* Parabolic Behaviour

$$s_0 = \frac{1}{d_1} \ln R.$$

Note that $C'(s) = -\lambda_1 A \exp(-\lambda_1 s) + \lambda_2 B \exp(-\lambda_2 s)$, hence, the c.f. always assumes the following minimum value:

$$s_m = \frac{1}{d_1} \ln(l_1 R). \tag{29}$$

Moreover, if $1 < l_1 < R^{1/m}$, the c.f. (16) always exhibits a behaviour which is linear in a neighborhood of the origin because: $\lim_{s \to 0^+} C'(s) = -\lambda_1 A + \lambda_2 B < 0$. Note that s_0 and s_m are independent from the dimension m of the Euclidean space $\mathbb{R}^m$.

In summary, through the difference between two exponential covariances as in (16), corresponding to models with the same parameter $\nu = 1/2$, parametric families able to fit various behaviours are available: models characterized just by positive values, along with models which provide negative values, along with models with a behaviour which could be linear or parabolic in a neighborhood of the origin. In the case the covariance models are always positive, this result does not depend on the dimension m of $\mathbb{R}^m$, as specified by inequality (13), unlike c.f.s with negative values that must satisfy inequality (14), which depends on the dimension m of $\mathbb{R}^m$.

Figure 1a displays the performance for the difference of two exponential models in the case that $1 < l_2 = R$, with the constraint $A - B = 1$. As previously underlined, this set of models, considering the above values of parameters, assumes only positive values and displays a behaviour which is parabolic in a neighborhood of the origin. The practical range is a growing function of the ratio l_2. Figure 1b displays the behaviour of the difference through exponential models in the case that $1 < l_2 < R$, with the constraints $C(0) = 1$, $A = 2, B = 1$ and $1 < l_2 < 2$. As previously underlined, this particular set of models assumes only positive values and this result is independent from the dimension m of $\mathbb{R}^m$. At last, the practical range is a growing function of the ratio l_2.

The solid lines of Fig. 1b display an upwards concavity since $1 < l_2 < \sqrt{R}$, hence the two solid lines do not exhibit any inflection point; conversely, the constraint $\sqrt{R} < l_2 < R$ is satisfied by the dash and dash-dot lines, hence they exhibit downwards concavity for $0 < s < s_F$, where s_F is the abscissa of the inflection point. In the extreme case $l_2 = R$, corresponding to the dot line, the c.f. exhibits a behaviour which is parabolic in a neighborhood of the origin, whereas the remaining four lines exhibit a behaviour which is linear in a neighborhood of the origin.

Figure 2a displays the behaviour for the difference of two exponential c.f.s for $m = 1$, with the constraint $1 < l_1 < R$, $C(0) = 1$, $A = 2, B = 1, \lambda_1 = 2$, for various values of λ_2, with the restriction $1 < l_1 < 2$. In accordance with (29), $s_m = \frac{1}{d_1} \ln 2l_1$ and $C(s_m) = \frac{\frac{1}{l_1} - 1}{(2l_1)^{\frac{1}{l_1 - 1}}}$: hence, as $l_1 \to 2$, $C(s_m)$ becomes even more negative. Likewise, the intersection point $s_0 = \frac{\ln 2}{d_1}$ with the s axis ($s > 0$) becomes ever greater as $d_1 \to 0$.

Figure 2b exhibits the results involving the difference of two exponential c.f.s for $m = 1$ when $1 < l_1 < R$ with the constraint $l_1 = 2, C(0) = 1$, i.e., $A - B = 1$. In accordance with (29), $s_m = \ln(2R)$, with $C(s_m) = \frac{-B^2}{4A}$. Hence, $C(s_m)$ becomes ever more negative by increasing the value of B. Likewise, the c.f. vanishes for $s_0 = \ln R$, hence s_0 becomes ever greater by getting B smaller and smaller.

- Considering the class defined in (18), the same family is always characterized by a behaviour which is parabolic in a neighborhood of the origin because:

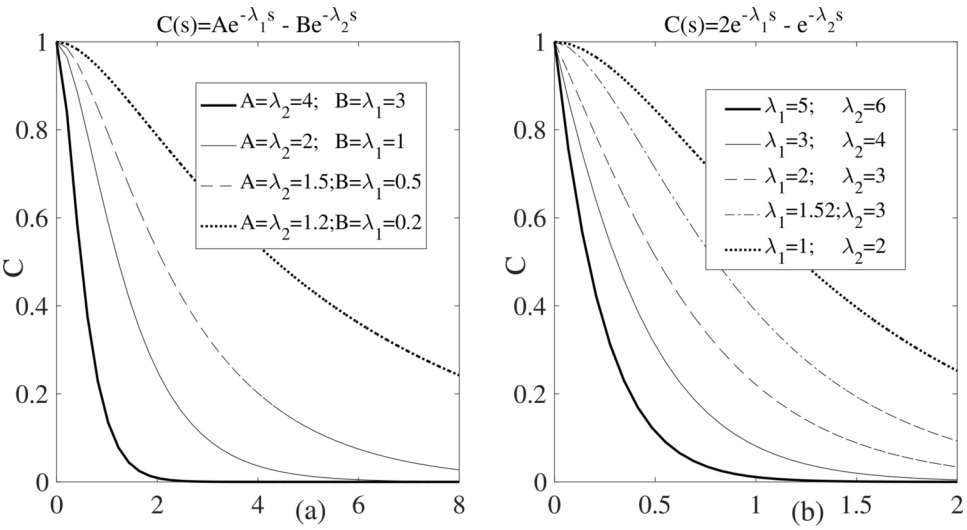

Fig. 1 Difference between two exponential c.f.s: **a** when $1 < R = l_2$, by fixing $A - B = 1$; **b** when $1 < l_2 < R$ by fixing $C(0) = 1, A = 2, B = 1$

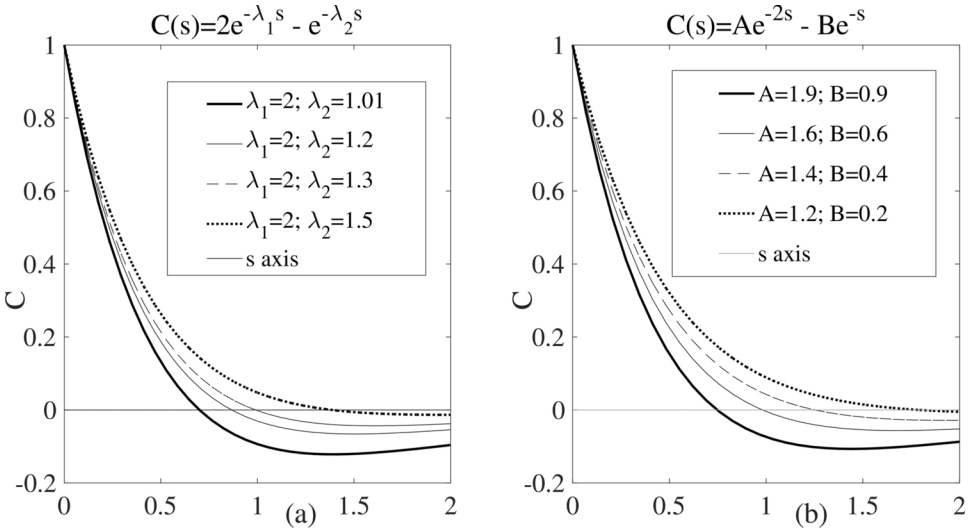

Fig. 2 Difference between exponential c.f.s ($m = 1$) with $1 < l_1 < R$: **a** $A = 2, B = 1, \lambda_1 = 2$, for different values of λ_2; **b** $\lambda_1 = 2, \lambda_2 = 1$, for different values of A and B, such that $A - B = 1$

$\lim_{s\to 0} C'(s) = 0$; moreover, it exhibits negative values if:

$$d_2|s| < \ln\left[\left(\frac{1}{R}\right)\left(\frac{\lambda_2 s+1}{\lambda_1 s+1}\right)\right];$$

however, if $1 < {l_2}^3 \leq R$, then

$$0 < \left[\left(\frac{1}{R}\right)\left(\frac{\lambda_2 s+1}{\lambda_1 s+1}\right)\right] < 1, \forall s > 0,$$

as a consequence the c.f. (18) cannot ever be negative. If $l_1 > 1$, then: $1 < l_1 < R^{1/m}$: in this case, it is straightforward to assess that the c.f. (18) assumes negative values for all $s \in \mathbb{R}$ such that:

$$d_1|s| > \ln\left[R\left(\frac{\lambda_1 s+1}{\lambda_2 s+1}\right)\right].$$

In summary, the difference of two c.f.s as in (18), corresponding to models with the same parameter $\nu = 3/2$, generates parametric families which present a behaviour which is parabolic in a neighborhood of the origin; moreover, in accordance with the values of the parameters, the same models could be always positive, as also there exist models which exhibit negative values as previously underlined. In the specific case the covariance models are always positive, this result does not depend on the dimension m of $\mathbb{R}^m$, as specified by inequality (13), unlike covariance models characterized by negative values which must satisfy inequality (14), which depends on the dimension m of $\mathbb{R}^m$. In Fig. 3a it is shown the behaviour of model (18) when $1 < {l_2}^3 < 2$, with $A = 2, B = 1$; as pointed out, in this case the covariance models are always positive and they are characterized by a parabolic behavior in a neighborhood of the origin: these results are independent from the dimension m of $\mathbb{R}^m$. Moreover, as the ratio l_2 becomes ever greater, the practical range becomes always bigger. Figure 3b displays the performance of model (18) which satisfies inequality (14), for the particular case $m = 1$, with $A = 1.5$ and $B = 0.5$, hence $1 < l_1 < 3$; as pointed out, in this case the covariance models are always negative in a subset of their domain and they are characterized by a parabolic behavior in a neighborhood of the origin. Note that as the difference d_1 increases, the intersection point with the s axis decreases.

- The covariance family (20) is always characterized by a behaviour which is parabolic in a neighborhood of the origin because $C'(0) = 0$ and it always exhibits negative values in a subset of its domain because the following inequality: $(\lambda_1^2 - \lambda_2^2)s^2 > \ln R$, is always satisfied for all $s > \sqrt{\frac{\ln R}{\lambda_1^2-\lambda_2^2}}$. At last, note that $C'(s) = 0$ for $s_m = \sqrt{\frac{\ln(l_1 R)}{\lambda_1^2-\lambda_2^2}}$ and $C''(s_M) > 0$, hence the above family always shows a minimum value. Figure 4a displays the behaviour of model (20), for the particular case $m = 2, \lambda_1 = 1.05, \lambda_2 = 1$, with $C(0) = 1$, i.e. $A - B = 1$; note that, as the ratio R increases, the intersection point with the s axis increases. Moreover, Fig. 4b displays the behaviour of model (20) for the particular case $m = 2, A = 5, B = 4$, with $C(0) = 1$, i.e. $A - B = 1$: as the difference d_1 increases, the intersection point with the s axis decreases. It is well known that the absolute minimum value of the cardinal sine model corresponds to -0.217 and it does not depend on the dimension of the Euclidean space. On the other hand, if correlation models with just one zero, a parabolic behaviour near the origin and negative values less than -0.217 are required, the new class of models given in (20) obtained through the difference of two Gaussian c.f.s, with the constraint given in (21), with $m = 1$, can be employed; for example, consider the following

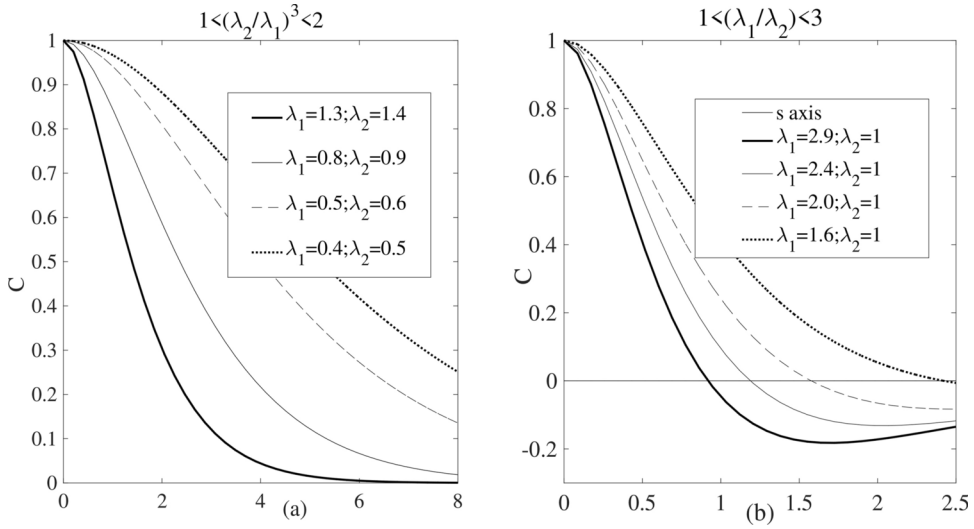

Fig. 3 Behaviour of model (18): **a** $1 < {l_2}^3 < 2$, with $A = 2, B = 1$;**b** $m = 1$, with $A = 1.5$ and $B = 0.5$ hence $1 < l_1 < 3$

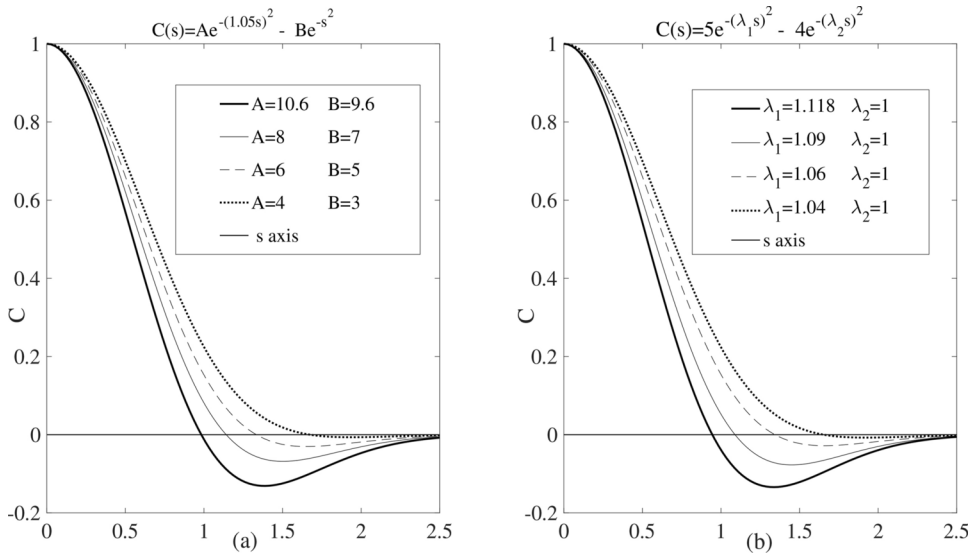

Fig. 4 Difference between two Gaussian c.f.s for $m = 2$: **a** $\lambda_1 = 1.05, \lambda_2 = 1$, by fixing $A - B = 1$, for different values of A and B, such that $1 < l_1 < R^{1/2}$; **b** $A = 5, B = 4$, for different values of λ_1 and λ_2, such that $1 < l_1 < R^{1/2}$

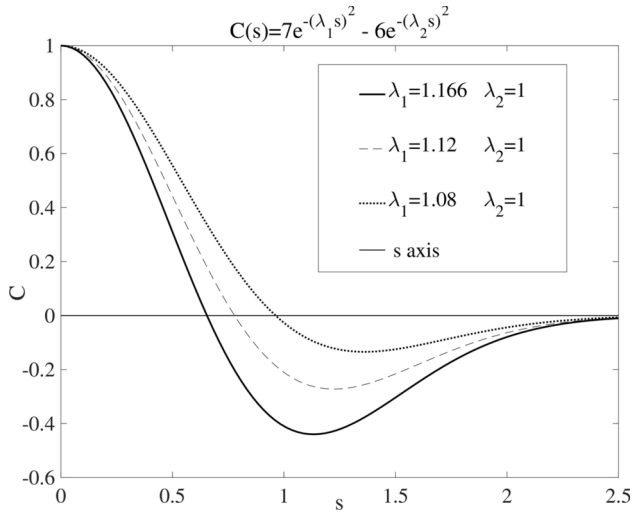

Fig. 5 Difference between two Gaussian models for $m = 1$, with $1 < l_1 < R$. Note that as the ratio l_1 becomes closer to R, the minimum value of the correlation model becomes more and more negative

subclass of the correlation family belonging to the class (20) where $\lambda_2 = 1$, and $A - B = 1$, represented in Fig. 5: note that as the ratio l_1 becomes closer to R, the absolute minimum value of the correlation model becomes more and more negative.

- All the results of Sect. 3.1, which can be very useful for practitioners for selecting appropriate correlation models, are summarized in Table 1. In summary, from the same results corresponding to models with the same parameter ν, it turns out that the conditions under which a c.f. is always positive do not depend on the dimension m of the Euclidean space $\mathbb{R}^m$, with respect to the conditions under which a c.f. is characterized by negative values in a subset of their domain; in this last case, the conditions depend on the dimension m of the Euclidean space $\mathbb{R}^m$.
- As previously underlined, the c.f.s described in Sect. 3.2 are given in terms of the variable $L = \lambda s$, hence the

values assumed by the same c.f.s do not depend on the parameter λ. In particular, the corresponding correlation functions will be considered hereafter, i.e., $C(0) = 1$.

- The correlation function ($C(0) = 1$) corresponding to the c.f. (23) can be written as follows:

$$C(L) = (1 - BL)\exp(-L), \quad B > 0; \tag{30}$$

according to (24) and to the constraint $A - B = 1$, the parameter B must satisfy the inequality:

$$B < \frac{1}{m}, \quad m = 1, 2, \ldots \tag{31}$$

The class (30) shows a behaviour which is linear in a neighborhood of the origin because $C'(0) < 0$; moreover, it always presents just one zero and it always displays negative values in the subset of its domain $\left]\frac{1}{B}, +\infty\right[$. The same class always exhibits a minimum value:

$$C(L_m) = \frac{-B}{\exp(1 + 1/B)}, \quad L_m = 1 + \frac{1}{B};$$

moreover, the absolute minimum value $C(L_m^*)$ of the family (30) can be easily computed as follows:

$$C(L_m^*) = \lim_{B \to (1/m)^-} \frac{-B}{\exp(1 + 1/B)} = \frac{-1}{m\exp(1 + m)}. \tag{32}$$

Figure 6 displays the behaviour of model (30) for the particular value $m = 1$: as B increases and approaches to 1, which is the threshold value of (31), the intersection point with the L axis decreases, whereas the minimum value of C becomes ever more negative and approaches to the absolute minimum value of (32), i.e., $C(L_1^*) = -\exp(-2) \approx -0.135$

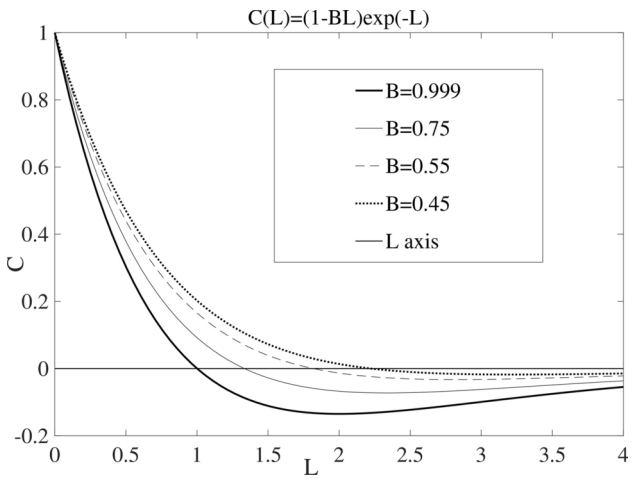

Fig. 6 Behaviour of model (30) for the particular value $m = 1$: as B increases and approaches to 1, which is the threshold value of (31), the intersection point with the L axis decreases, whereas the minimum value of C becomes ever more negative and approaches to the absolute minimum value of (32), i.e., $C(L_1^*) = -\exp(-2) \approx -0.135$

which is the threshold value of (31), the intersection point with the L axis decreases, whereas the minimum value of C becomes ever more negative and approaches to the absolute minimum value of (32), i.e.,

$$C(L_1^*) = -\exp(-2) \approx -0.135.$$

- The correlation function ($C(0) = 1$) corresponding to the c.f. (25) can be written as follows:

$$C(L) = (1 - 3BL - BL^2)\exp(-L), \qquad B > 0; \tag{33}$$

according to (26) and to the constraint $A - 3B = 1$, the parameter B must satisfy the inequality:

$$B < \frac{1}{m(m+4)} \quad m = 1, 2, \ldots \tag{34}$$

The class (33) shows a behaviour which is linear in a neighborhood of the origin because $C'(0) < 0$; moreover, it always presents just one zero ($L_0 > 0$) and it always displays negative values in the subset of its domain $\left]L_0, +\infty\right[$, where $L_0 = \frac{-3+\sqrt{9+\frac{4}{B}}}{2} > 0$. Note that for the family (33) $C' = 0 \iff BL^2 + BL - 3B - 1 = 0$, hence the minimum value $C(L_m)$ is obtained for $L_m = \frac{-1+\sqrt{\frac{4}{B}+13}}{2}$. Moreover, the absolute minimum value $C(L_m^*)$ of the family (33) can be easily computed as follows:

$$C(L_m^*) = \lim_{B \to [m(m+4)]^{-1}} \left[(1 - 3BL_m - BL_m^2)\exp\left(-L_m\right)\right] =$$

$$= \left[1 - \frac{3g(m)}{2m(m+4)} - \frac{[g(m)]^2}{4m(m+4)}\right]\exp\left[\frac{-g(m)}{2}\right], \tag{35}$$

where $g(m) = \left(\sqrt{4m^2 + 16m + 13} - 1\right)$. Figure 7 displays the behaviour of model (33) for the particular value $m = 1$: as B increases and approaches to 0.2, which is the threshold value of (34), the intersection point with the L axis decreases, whereas the minimum value of C becomes ever more negative and approaches to the absolute minimum value of (35), i.e., $C(L_1^*) \approx -0.144$.

- In summary, the difference of an exponential model with a c.f. obtained as the product of a polynomial of degree $n = 1$ or $n = 2$ with an exponential, as specified in Eqs. (23) and (25), corresponding to models with the same λ, always yields c.f.s with a linear behaviour in a neighborhood of the origin and they are always negative in a subset of their domain, as previously underlined.

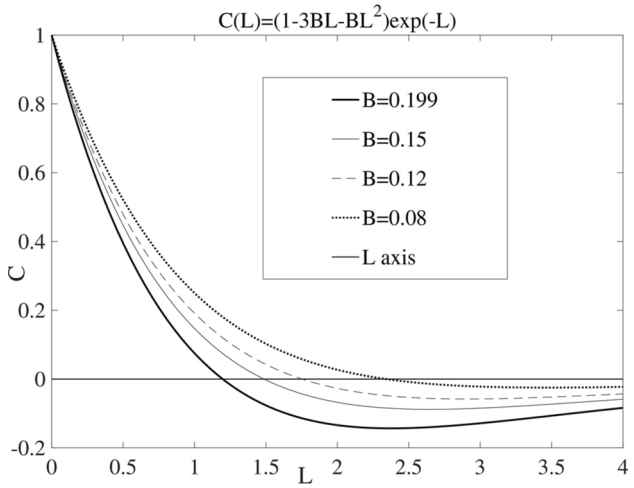

Fig. 7 Behaviour of model (33) for the particular value $m = 1$: as B increases and approaches to 0.2, which is the threshold value of (34), the intersection point with the L axis decreases, whereas the minimum value of C becomes ever more negative and approaches to the absolute minimum value of (35), i.e., $C(L_1^*) \approx -0.144$

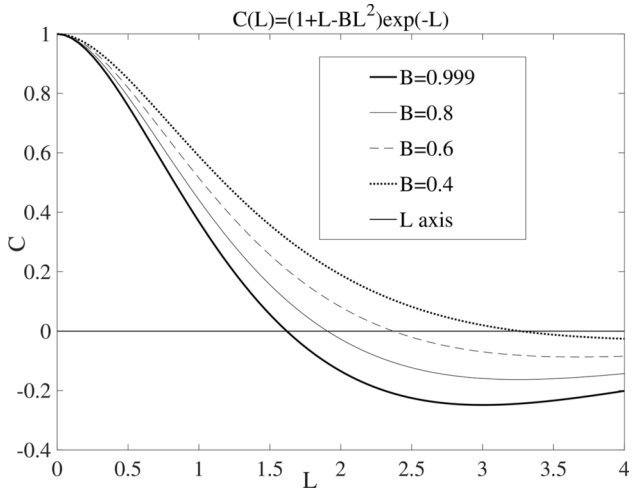

Fig. 8 Behaviour of model (36) for the particular value $m = 1$: as B increases and approaches to 1, which is the threshold value of (37), the intersection point with the L axis decreases, whereas the minimum value of C becomes ever more negative and approaches to the absolute minimum value of (38), i.e., $C(L_1^*) = \frac{-5}{e^3} \approx -0.25$.

Moreover, these c.f.s always satisfy inequality (15), hence the admissibility condition depends on the dimension m of the Euclidean space $\mathbb{R}^m$.

- The correlation function ($C(0) = 1$) corresponding to the c.f. (27) can be written as follows:

$$C(L) = (1 + L - BL^2)\exp(-L), \quad B > 0; \tag{36}$$

according to (28) and to the constraint $A - 3B = 1$, the parameter B must satisfy the inequality:

$$B < \frac{1}{m} \quad m = 1, 2, \ldots \tag{37}$$

The class (36) shows a behaviour which is parabolic in a neighborhood of the origin because $C'(0) = 0$; moreover, it alaways presents just one zero ($L_0 > 0$) and it always displays negative values in the subset of its domain $]L_0, +\infty[$, where

$$L_0 = \frac{1 + \sqrt{1 + 4B}}{2B} > 0.$$

Note that for the family (36) $C' = 0 \Longleftrightarrow L(BL - 2B - 1) = 0$, hence the same class always exhibits a minimum value:

$$C(L_m) = \frac{-1 - 4B}{\exp(2 + 1/B)}, \quad L_m = 2 + \frac{1}{B};$$

in particular, the absolute minimum value $C(L_m^*)$ of the family (36) can be easily computed as follows:

$$C(L_m^*) = \lim_{B \to (1/m)^-} \frac{-1 - 4B}{\exp(2 + 1/B)} = \frac{-m - 4}{m\exp(2 + m)}. \tag{38}$$

Figure 8 displays the behaviour of model (36) for the particular value $m = 1$: as B increases and approaches to 1, which is the threshold value of (37), the intersection point with the L axis decreases, whereas the minimum value of C becomes ever more negative and approaches to the absolute minimum value of (38), i.e.,

$$C(L_1^*) = \frac{-5}{e^3} \approx -0.25.$$

- From the results of Sect. 3.2, summarized in Table 2, corresponding to models with the same parameter λ, it turns out that all the models are always characterized by negative values in a subset of their domain; hence, as in the previous case, the conditions depend on the dimension m of the Euclidean space $\mathbb{R}^m$.
- As it has been shown, the proposed families of c.f.s present easy expressions, hence they can be easily managed from the computational perspective. As previously underlined, most of the classes of c.f.s utilized in the literature are always positive (Cressie and Huang 1999; De Iaco et al. 2002a; Gneiting 2002; De Iaco et al. 2002b), hence they fail to handle negative correlations.

5 Conclusions

In the present paper the difference between two Whittle–Matérn c.f.s has been analyzed: these results provide a further development and generalization, valid for any dimension m of the Euclidean space $\mathbb{R}^m$, of the ones given in Posa (2023). In particular, the new families obtained through the above difference present interesting features, since they are able to model several correlation structures characterized by different behaviours. Indeed, they are capable to describe negative and positive correlations, as well as several behaviours near the origin by properly adapting the parameters on which they depend. As underlined throughout the paper, all the traditional hole effect models stem from the Bessel family and they are characterized by the same features, i.e., they present a countable infinity of zeros and a parabolic behaviour near the origin. On the other hand, the models proposed in this paper are characterized by a complementary behaviour, which cannot be detailed by all the classical hole effect correlation models: they are essentially characterized by just one zero, moreover they are able to describe various behaviours near the origin (linear and parabolic), as well as different behaviours concerning the concavity in proximity of the origin (upwards and downwards). Taking into account the analysis provided in this paper, the outcoming results can be particularly useful for many practitioners.

Acknowledgements The author is very grateful to the editor and the referees for their useful comments and precious suggestions, which contributed to improve the previous version of the paper.

Funding Open access funding provided by Università del Salento within the CRUI-CARE Agreement.

References

Alegria A, Ramirez F, Porcu E (2024) Hybrid parametric classes of isotropic covariance functions for spatial random fields. Math Geosci 41:100491

Apanasovich TV, Genton MG (2010) Cross-covariance functions for multivariate random fields based on latent dimensions. Biometrika 97:15–30

Apanasovich TV, Genton MG, Sun Y (2012) A valid Matérn class of cross-covariance functions for multivariate random fields with any number of components. J Am Stat Assoc 107:180–193

Asghari O (2015) Geostatistical simulation of dyke systems in sungun porphyry copper deposit, Iran. J Min Environ 6(1):1–10

Batchelor GK (1982) The theory of homogeneous turbolence. Cambridge University Press, Cambridge, p 197

Bochner S (1959) Lectures on Fourier integrals. Princeton University Press, Colorado, p 333

Chilès J, Delfiner P (1999) Geostatistics. Probability and statistics series. Wiley, New York, p 687

Cressie N, Huang H (1999) Classes of nonseparable, spatio-temporal stationary covariance functions. J Am Stat Assist 94(448):1330–1340

Creutin JD, Obled C (1982) Objective analysis and mapping techniques for rainfall fields: an objective comparison. Water Resour Res 18:413–431

De Iaco S, Myers D, Posa D (2002) Nonseparable space-time covariance models: some parametric families. Math Geol 34(1):23–41

De Iaco S, Myers D, Posa D (2002) Space-time variograms and a functional form for total air pollution measurements. Comput Stat Data Anal 41(2):311–328

Faouzi T, Porcu E, Kondrashuk I, Bevilacqua M (2022) Convergence arguments to bridge Cauchy and Matérn covariance functions. Stat Pap 13(2):1–16

Gneiting T (2002) Nonseparable, stationary covariance functions for space-time data. J Am Stat Assist 97(458):590–600

Gregori P, Porcu E, Mateu J, Sasvári Z (2008) On potentially negative space time covariances obtained as sum of products of marginal ones. Ann Inst Stat Math 60:865–882

Griffith DA (2019) Negative spatial autocorrelation: one of the most neglected concepts in spatial statistics. Stats 2:388–415

Guinness J (2022) Inverses of Matérn covariances on grids. Biometrika 109(2):535–541

Guttorp P, Gneiting T (2006) Studies in the history of probability and statistics XLIX on the Matérn correlation family. Biometrika 93(4):989–995

Handcock MS, Stein ML (1993) A Bayesian analysis of kriging. Technometrics 35(4):403–410

Hristopulos DT (2015) Covariance functions motivated by spatial random field models with local interactions. Stoch Environ Res Risk Assess 29:739–754

Hristopulos DT (2020) Random fields for spatial data modeling. A primer for scientists and engineers. Series in advances in geographic information science. Springer, Berlin

Hristopulos DT (2024) Non-separable covariance kernels for spatio-temporal Gaussian processes based on a hybrid spectral method and the harmonic oscillator. IEEE Trans Inf Theory. https://doi.org/10.1109/TIT.2023.3321215

Hu L, Griffith DA, Chun Y (2018) Space-time statistical insights about geographic variation in lung cancer incidence rates: Florida, USA, 2000–2011. Environ Res Public Health 15:1–18

Jones RH (1989) An approach to producing space-time covariance functions on spheres. Stoch Hydrol Hydraul 3:100–105

Journel AJ, Froidevaux R (1982) Anisotropic hole-effect modeling. Math Geol 14(3):217–239

Kamash KAM, Robson JD (1978) The applications of isotropy in road surface modelling. J Sound Vib 57(1):89–100

Levinson SJ, Beall JM, Powers EJ, Bengtson RD (1984) Space-time statistics of the turbulence in a tokamak edge plasma. Nucl Fusion 24:527–540

Lindgren F, Rue H, Lindstrom J (2011) An explicit link between gaussian fields and gaussian Markov random fields: the stochastic partial differential equation approach. J Roy Stat Soc B 73(4):423–498

Longuet-Higgins MS (1957) Statistical properties of an isotropic random surface. Philos Trans R Soc A250:157–174
Ma C (2005) Linear combinations of space-time covariance functions and variograms. IEEE Trans Signal Process 53(3):857–864
Ma YZ, Jones TA (2001) Modeling hole-effect variograms of lithology-indicator variables. Math Geol 33(5):631–648
Matérn B (1980) Spatial variation. Lecture notes in statistics (2nd ed), vol 151. Springer, New York, p 36. 1st ed 1960 published in Meddelanden fran Statens Skogsforskningsinstitute Swed., 49(5)
Meija JM, Rodriguez-Iturbe I (1974) On the synthesis of random field sampling from the spectrum: an application to the generation of hydrological spatial processes. Water Resour Res 66:705–711
Polya G (1949) Remarks on characteristic functions. In: Proceedings of the 4th Berkeley symposium mathematics statistics and propagation. University of California Press, Berkeley, pp 115–123
Pomeroy JW, Toth B, Granger RJ, Hedstrom NR, Essery RLH (2003) Variation in surface energetics during snowmelt in a subarctic mountain catchment. J Hydrometeorol 4:702–719
Porcu E, Bevilacqua M, Schaback R, Oates CJ (2024) The Matérn model: a journey through statistics, numerical analysis and machine learning. Stat Sci 39(3):469–492
Posa D (2021) Models for the difference of continuous covariance functions. Stoch Env Res Risk Assess 35:1369–1386
Posa D (2023) Special classes of isotropic covariance functions. Stoch Environ Res Risk Assess 37:1615–1633
Schoenberg IJ (1938) Metric spaces and completely monotone functions. Anal Math 39(4):811–841
Shkarofsky IP (1968) Generalized turbulence space-correlation and wave-number spectrum-function pairs. Can J Phys 46:2133–2153
Stein ML (1999) Interpolation of spatial data. Springer Series in Statistics. Springer, New York, p 247
Wang S, Abdulah S, Sun Y, Genton MG (2023) Which parameterization of the Matérn covariance function? Spat Stat 58:100787
Whittle P (1954) On stationary processes in the plane. Biometrika 41:434–449
Xu ZW, Wu J, Wu ZS (2003) Statistical temporal behaviour of pulse wave propagation through continuous random media. Waves Random Media 13:59–73
Xu ZW, Wu J, Huo WP, Wu ZS (2003) Temporal skewness of electromagnetic pulsed waves propagating through random media with embedded irregularity slab. Chin Phys Lett 20:370–373
Yaglom AM (1987) Correlation theory of stationary and related random functions: basic results. Springer, New York, p 526
Yakhot V, Orszag SA, She ZS (1989) Space-time correlations in turbulence—kinematical versus dynamical effects. Phys Fluids 1:184–186
Ye J, Lazar NA, Li Y (2015) Nonparametric variogram modeling with hole effect structure in analyzing the spatial characteristics of fmri data. J Neurosci Methods 240:101–115